Broadband detection of methane and nitrous oxide using a distributed-feedback quantum cascade laser array and quartz-enhanced photoacoustic sensing

Marilena Giglio[a,b], Andrea Zifarelli[b], Angelo Sampaolo[a,b], Giansergio Menduni[b,c],
Arianna Elefante[b], Romain Blanchard[d], Christian Pfluegl[d], Mark F. Witinski[d],
Daryoosh Vakhshoori[d], Hongpeng Wu[a], Vittorio M.N. Passaro[c], Pietro Patimisco[a,b],
Frank K. Tittel[e], Lei Dong[a,*], Vincenzo Spagnolo[a,b,*]

[a] *State Key Laboratory of Quantum Optics and Quantum Optics Devices, Institute of Laser Spectroscopy, Shanxi University, Taiyuan 030006, China*
[b] *PolySense Lab – Dipartimento Interateneo di Fisica, Politecnico and University of Bari, CNR-IFN, Via Amendola 173, Bari, Italy*
[c] *Photonics Research Group, Dipartimento di Ingegneria Elettrica e dell'informazione, Politecnico di Bari, Via Orabona 4, Bari, 70126, Italy*
[d] *Pendar Technologies, 30 Spinelli Place, Cambridge, MA, 02138, USA*
[e] *Rice University, Department of Electrical and Computer Engineering, 6100 Main Street, Houston, TX, 77005, USA*

ARTICLE INFO

ABSTRACT

Here we report on the broadband detection of nitrous oxide (N_2O) and methane (CH_4) mixtures in dry nitrogen by using a quartz-enhanced photoacoustic (QEPAS) sensor exploiting an array of 32 distributed-feedback quantum cascade lasers, within a spectral emission range of $1190-1340 \text{ cm}^{-1}$ as the excitation source. Methane detection down to a minimum detection limit of 200 ppb at 10 s lock-in integration time was achieved. The sensor demonstrated a linear response in the range of $200-1000$ ppm. Three different mixtures of N_2O and CH_4 in nitrogen at atmospheric pressure have been analyzed. The capability of the developed QEPAS sensor to selectively determine the N_2O and CH_4 concentrations was demonstrated, in spite of significant overlap in their respective absorption spectra in the investigated spectral range.

1. Introduction

Gas spectroscopy finds applications in breath analysis, industrial process control, environmental monitoring, geochemistry and leak detection [1–3]. Spectroscopic techniques capable of implementing wide spectral range analysis allow the detection of broadband absorber gases, such as greenhouse and volatile organic compounds, and measurements of complex gas mixtures of interfering components [4]. Among the optical sensing techniques, photoacoustic spectroscopy (PAS) and quartz-enhanced photoacoustic spectroscopy (QEPAS) are particularly suitable for broadband detection since the responsivity of the employed detecting element is wavelength-independent. In PAS the acoustic waves generated by the non-radiative relaxation of the gas target molecules excited by a modulated laser light are detected by a sensitive microphone. Typically, the PAS signal is amplified by tuning the modulation frequency to one of the acoustic resonances of the photoacoustic cell [5]. In QEPAS a quartz tuning fork (QTF) is

employed as a sharply resonant acoustic transducer and the QEPAS signal is amplified by modulating the laser light at one of the in-plane flexural modes of the QTF [6]. Both techniques have demonstrated high sensitivity in concentration [5–9]. Typically, single mode distributed-feedback (DFB) diode lasers have been employed as a light source to target a single, interference-free absorption line, thus demonstrating high selectivity. Apart from specific cases in which two or more absorption lines can be covered within its dynamic current range [10,11], DFB lasers do not represent the optimal choice for multi-gas detection. Quantum cascade lasers (QCLs) in external-cavity configuration (EC-QCLs) are commonly employed to cover wide mid-infrared spectral ranges and have been exploited for the detection of several greenhouse and harmful gases [12]. For broadband gas detection (over a $\sim 40 \text{ cm}^{-1}$ wide spectral range), EC-QCLs have been employed for acetylene and TNT detection with PAS [13] and for Freon 125 detection with a QEPAS sensor [14]. Compared to DFB laser sources, EC-QCLs are bulky and suffer from grating mechanical instability which generates alignment-

---

and laser instability-related noise signals [15]. An alternative broadband emission laser source can be realized by using an array of DFB-QCLs monolithically grown on a single semiconductor chip, combining the compactness of a single chip, the wide tunability range of an array of devices and the pulse-to-pulse stability, spectral purity, and tuning reproducibility of DFB-QCLs [16]. Recently, a DFB-QCL array with 32 DFB-QCLs was employed as the excitation source in a QEPAS sensor for broadband detection of N_2O at atmospheric pressure in the $1190 - 1340$ cm^{-1} spectral range, with a sensitivity suitable for atmospheric monitoring [17,18]. In the investigated spectral range, N_2O exhibits two ~50 cm^{-1} wide absorption bands composed of several ~1 cm^{-1} equally separated absorption lines whose smooth envelope results in a P- or R- branch [19,20].

In this work, we investigated the performance of the DFB-QCL array-based QEPAS sensor in the detection of methane (CH_4) to test the sensor capability to detect and recognize the absorption features of a gas presenting an irregular spectrum within the source emission spectral range [21]. The feasibility of broadband multi-gas detection was investigated, by analyzing mixtures of N_2O and CH_4 with strongly overlapping absorption bands. To avoid the influence of water vapor on the analytes energy relaxation rate [22], altering the spectra intensity, all measurements were performed in pure, non-humidified N_2. Our analysis demonstrated the capability of discriminating the contributions of a gas species from another one, even in the case of strongly overlapping absorption spectra. A quantitative estimation of the concentrations of the two gas species in the mixture was obtained by fitting spectra of mixtures with a linear combination of reference spectra of N_2O and CH_4, at a fixed concentration in N_2.

2. Laser source spectral characterization and beam profile analysis

The employed laser source consists in a monolithic array of 32 individually addressable distributed-feedback quantum cascade lasers grown on a single semiconductor chip and operated in pulsed mode, as described in [15,17,21]. Thermoelectric cooler and laser pulser boards are embedded in a single unit controlled by a LabVIEW-based software.

As a first step, the spectral emission of the employed laser source was analyzed by using a Fourier-transform interferometer (FTIR-Nicolet 6700) with a spectral resolution of 0.125 cm^{-1} in a rapid-scan mode. In Fig. 1(a) the normalized emission spectra of the devices composing the monolithic QCL array are reported for a TEC temperature of 25 °C, a drive voltage properly set for each device in order to ensure the highest optical power output (18.0–20.0 V), a repetition frequency of 33 kHz and a pulse-width of 300 ns resulting in a duty cycle of 1 %.

The overall emission spectrum of the QCL array covers a range 150 cm^{-1} wide from 1190 cm^{-1} to 1340 cm^{-1}. Each device in the array shows a single-mode output, whose peak emission wavenumber and linewidth were determined by fitting the spectrum with a Gaussian curve. As a representative, the FTIR measured spectrum of the QCL number 15 is reported at a driving voltage of 18 V in Fig. 1(b) together with its best Gaussian fit. The emission peak occurs at 1253.4 cm^{-1} with a linewidth of 1.3 cm^{-1}. By repeating the measurements and the fit procedure for all the QCLs, a spectral spacing between adjacent devices lower than 5 cm^{-1} was measured, while the linewidths ranged between 1.1 cm^{-1} and 1.5 cm^{-1}. Narrower spectral lines (down to < 0.2 cm^{-1}) can be obtained by reducing the pulse durations. However, this also leads to a reduction of the average power if the repetition rate is kept constant to match the resonance of the quartz tuning fork. Since the QEPAS signal is proportional to laser average power, this is not advantageous. Mode hop-free tuning of the lasers' optical frequency with the operating temperature was also verified in the 15 °C–50 °C range. The temperature tuning coefficient was calculated by linearly fitting the peak wavenumber as a function of the operating temperature. The optical frequency temperature tuning of the device number 15 is reported in Fig. 1(c) together with the best linear fit. A tuning coefficient of -0.09 cm^{-1}/°C was measured for all the devices in the array, resulting in an overall tuning of each QCL optical frequency of 3.15 cm^{-1} within the investigated temperature range. Next the spatial quality of the QCL beams was investigated. The beams exiting the QCL array package were collected by a ZnSe focusing lens having a 25.4 mm diameter, a 50 mm focal length and an anti-reflection (AR) coating in the $7 - 12$ μm spectral range. The beam profile of each device was acquired in the lens focal plane by a pyroelectric camera (Ophir Spiricon Pyrocam III-C) composed of an array of 124×124 100μm-side square pixels. Devices from number 1 to number 19 shown on the camera a secondary spot, ~ 1 mm distant from the fundamental one, caused by stray light in the laser package. An updated design is currently being engineered to mitigate this issue. As representative, the three-dimensional far field image of the device number 15 is shown in Fig. 2(a). The secondary spot is 6 times less intense and appears 900 μm far from the highest peak.

In an on-beam QEPAS configuration, the laser source beam must be focused between the QTF prongs. When light hits the QTF prongs a background optical noise is generated. Therefore, multimode and/or poor spatial quality beams drastically affect the ultimate detection sensitivity of a QEPAS sensor. With the QCL array employed in this work, a spatial filter was used to suppress all secondary spots. Although hollow-core waveguides (HCWs) have been demonstrated to act as efficient low-loss single mode delivery spatial filters in the mid-infrared
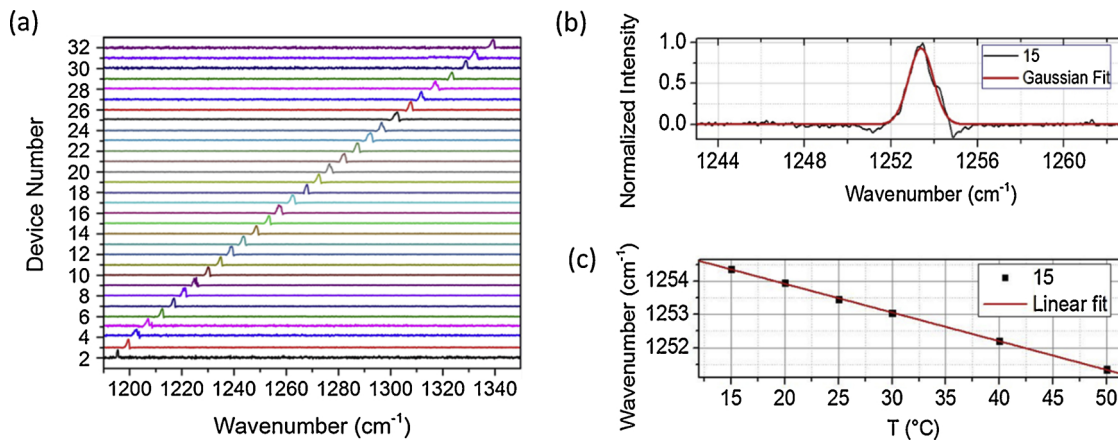

Fig. 1. (a) QCL array FTIR normalized intensity spectra for a 25 °C operating temperature, a 33 kHz repetition frequency, a 300 ns pulse-width and a driving voltage maximizing the devices optical power; (b) Gaussian fit (red solid line) of the normalized emission spectrum (black solid line) and (c) linear fit (red solid line) of temperature tuning of the peak emission wavelength (black dots) for the DFB-QCL number 15.
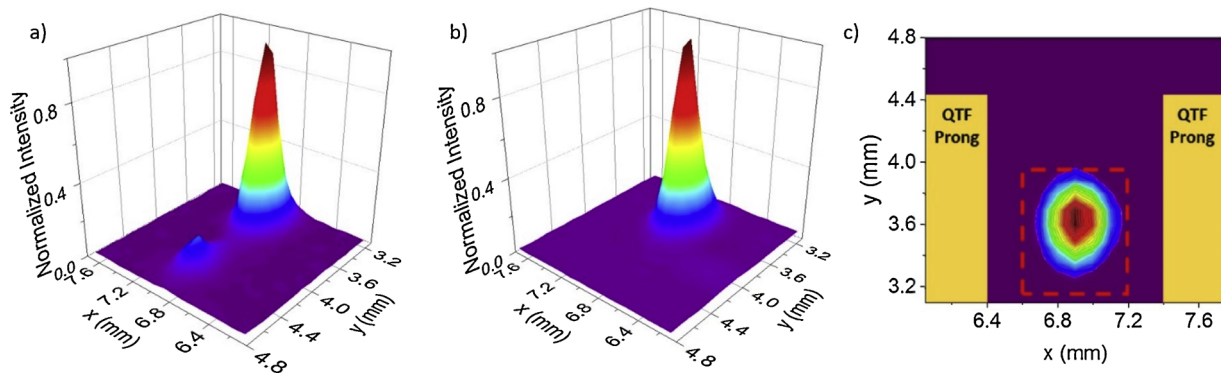
Fig. 2. (a) QCL number 15 focused 3D beam profile. (b) Same QCL beam profile filtered by a 2-mm pinhole. (c) QCL number 15 2D spatially filtered beam profile. The two yellow areas represent the positions of the QTF prongs, spaced by 1-mm. The array overall illuminated area is highlighted with a red dashed line. All dimensions are represented in scale.

spectral range, the observed shifts of the focused beams when switching from one device to another do not permit the use of an HCW, since realignments become necessary when switching the QCLs [23,24]. Instead, a 2 mm-diameter pinhole was positioned between the laser source and the focusing lens, allowing all the secondary spots to be cut off while preserving the fundamental mode Gaussian shape and intensity, as shown in Fig. 2(b) for device 15. Once the secondary spots are removed, beam radii of 260–300 μm in the x-direction and of 290–340 μm in the y-direction were measured in the lens focal plane by fitting all beam profiles with a Gaussian function in both directions. By considering also shifts in position of all primary spots, an overall illuminated area of $600 \times 800 \ \mu m^2$ was identified, represented by a dashed line-rectangle in Fig. 2(c). Hence, a 1 mm-prong spacing custom QTF (labelled as QTF#4 in [25]) was selected to reduce as much as possible the possibility that beam tails hit the QTF.

3. Experimental setup

The architecture of the broadband detection QEPAS sensor is depicted in Fig. 3. As discussed in the previous section, the laser beam is spatially filtered by a pinhole and then focused through the acoustic detection module (ADM) by means of the ZnSe focusing lens.

The ADM is composed of a gas cell, equipped with two ZnSe windows for the laser input and output, a pair of connectors for gas inlet and outlet and a QTF acoustically coupled with two 1.52 mm-internal diameter and 5.3 mm-long micro-resonator tubes in an on-beam configuration. A power-meter is set behind the ADM for optical power measurement and monitoring. At atmospheric pressure, the spectrophone composed of a QTF and micro-resonator tubes exhibits a first overtone flexural mode resonance curve peaked at $f = 25,390.63 \ Hz$ with a full-width half-maximum value of 2.41 Hz, resulting in a quality factor of 10,530. The laser pulser is externally triggered by a waveform generator to set the pulse repetition rate at f. For all QEPAS measurements, a 300 ns pulse-width was used, resulting in a 0.75 % duty cycle, while the QCL driving voltage was set to the value ensuring the highest optical power for each device. The QTF current signal is converted into a voltage signal by a 10 MΩ feedback resistor pre-amplifier and then demodulated by a lock-in amplifier at the frequency f with a 100 ms integration time. The demodulated signal is digitized by a DAQ card and acquired by a LabVIEW-based software with a sampling time of
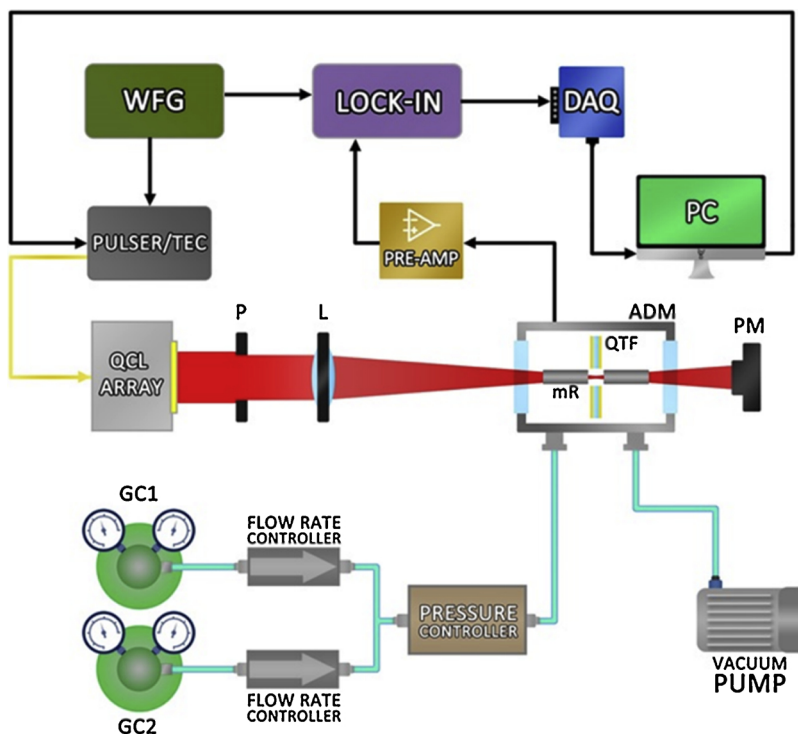

Fig. 3. Schematic of the experimental apparatus. WFG – waveform generator; DAQ – data acquisition board; TEC – temperature controller; PRE-AMP – Pre-amplifier; PC – personal computer; QCL ARRAY – quantum cascade laser array; P – pinhole; L – focusing lens; ADM - acoustic detection module; QTF – quartz tuning fork; mR – micro-resonator tubes; PM – power-meter; GC1, GC2 – gas cylinders.

300 ms.

The target gas flows from the gas cylinder GC1 through the ADM by using a vacuum pump. The gas flow rate and pressure in the ADM are set by controllers at 30 sccm and 760 Torr, respectively. A hygrometer (not shown in figure) was placed in-line to monitor the absence of humidity in the line and check any presence of undesired water vapor. Gas mixtures with a second gas species contained in the gas cylinder GC2 are obtained by appropriate setting the rate parameter of the flow controllers mounted on the two branches of the Y-shaped gas line.

4. Methane broadband detection

Within the emission wavelength range of the employed DFB-QCL array, methane exhibits an uneven absorption spectrum composed of several lines differing both in line-strength and in wavenumber spacing. QEPAS measurements were performed by switching the QCLs in sequence while keeping the devices operating temperature fixed at 25 °C (fixed temperature acquisition mode-FTAM). All measurements were performed by using the lock-in phase $\varphi = 57.3°$, maximizing the demodulated signal amplitude of the methane peaks. The QCL output power varies for each device. For this reason, a preliminary measurement of the array optical power was performed as a function of light wavenumber, by recording the output power while switching the devices in sequence. The obtained curve was then normalized to 1 with respect to the highest value. This curve will be referred hereafter as FTAM optical power calibration curve. QEPAS signals obtained for a certified concentration of 1000 ppm of $CH_4:N_2$ in GC1 were normalized to the FTAM optical power calibration curve. The resulting QEPAS spectrum is shown in Fig. 4 (black squares).

The FTAM QEPAS spectrum reproduces the highest intensity peak at 1306.10 cm^{-1} as well as several side features. For each device, a 1σ noise level of ~ 2 μV was estimated when pure N_2 is flowing in the ADM. This suggests that the background optical noise related to light-induced photothermal effects on QTF prongs does not change when switching between different devices. Therefore, the selected QEPAS sensor architecture, i.e. the use of the pinhole together with a 1mm-prong spacing QTF, allows the QEPAS sensor alignment conditions to be preserved while switching among the devices.

The QEPAS sensor linear responsivity with the methane concentration was verified in the $200-1000$ ppm range, by diluting the 1000 ppm $CH_4:N_2$ certified concentration with pure nitrogen. The measurements obtained in fast acquisition mode for 400, 600, 800 and

1000 ppm CH_4 concentrations are shown in Fig. 4, together with the spectra recorded when pure N_2 was flowing in the ADM. The area underneath the spectra was calculated using the rectangles approximation and plotted as a function of the CH_4 concentration in the inset of Fig. 4. A slope of 0.036 mV·cm^{-1}/ppm was extracted by linearly fitting the data points in the graph. The fit exhibits an intercept of 1.74 mV·cm^{-1}, comparable with the area of 2.6 mV·cm^{-1} measured underneath the pure nitrogen QEPAS spectrum. For the lowest concentration, i.e. 200 ppm $CH_4:N_2$, an area of 7.87 mV·cm^{-1} was calculated. The standard deviation σ_{Area} of the area underneath the QEPAS spectrum can be obtained by using the propagation of uncertainty law:

$$\sigma_A = \sqrt{\sum_i \left[\left(\frac{\partial A}{\partial x_i}\right)^2 \sigma_{x_i}^2 + \left(\frac{\partial A}{\partial S_i}\right)^2 \sigma_{S_i}^2 \right]} \tag{1}$$

where x_i and S_i are the ith rectangle base and height. The parameter σ_{x_i} is the FTIR error, while σ_{S_i} is the 1σ noise of the QEPAS signal. The QEPAS signal for each QCL exhibits a 1σ noise level of ~ 2 μV. By neglecting the FTIR error contribution, σ_{Area} is proportional to 1σ and the extracted value is 0.05 mV·cm^{-1}. The sensor minimum detection limit (MDL) can be defined as the methane concentration corresponding to an area under the spectrum equal to σ_{Area}. Based on these considerations, an MDL of 1.27 ppm was estimated. 1σ noise of the QEPAS signal can be further reduced by integrating the signal over longer times. An Allan-Werle deviation analysis was performed to calculate 1σ noise as a function of the signal integration time [26]. For a 10 s lock-in integration time, the methane MDL was estimated to improve down to 200 ppb, ~ 9 times lower than the methane concentration in atmosphere [27].

The methane spectrum was also measured by employing a higher-resolution acquisition mode which consists in tuning the operating temperature of each QCL within the 15 °C–50 °C range, in steps of 3 °C, corresponding to a spectral resolution of 0.27 cm^{-1}, and driving the devices one by one, in sequence (temperature tuning acquisition mode-TTAM). A preliminary measurement of the TTAM optical power calibration curve was performed. QEPAS signals obtained for a certified concentration of 1000 ppm of $CH_4:N_2$ in GC1 were normalized to the TTAM optical power calibration curve. The resulting QEPAS spectrum is shown in Fig. 5 (black dots) together with a simulation of the absorption spectrum of 1000 ppm of $CH_4:N_2$ obtained by using the HITRAN database [28].

QEPAS measurements well reconstruct the highest intensity peak centered at 1306.10 cm^{-1}. Compared to Fig. 4, five equally spaced absorption features on the right side of the highest peak are now distinguishable and well reconstructed. However, the large QCLs emission linewidth, combined with the ~ 5 cm^{-1} spacing and the $1-4$ cm^{-1} width of the methane absorption peaks, results in a QEPAS spectrum less
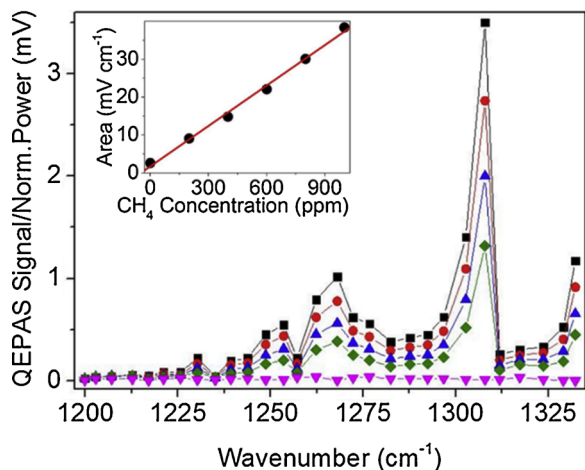

Fig. 4. 1000 ppm (black squares), 800 ppm (red dots), 600 ppm (blue triangles) and 400 ppm (green diamonds) $CH_4:N_2$ and pure N_2 (pink triangles) FTAM QEPAS signal normalized to the optical power calibration curve. Solid lines are visual guides. Inset: Area underneath the QEPAS spectrum in mV·cm^{-1} units measured for each $CH_4:N_2$ concentration (black dots) and corresponding best linear fit (red line).
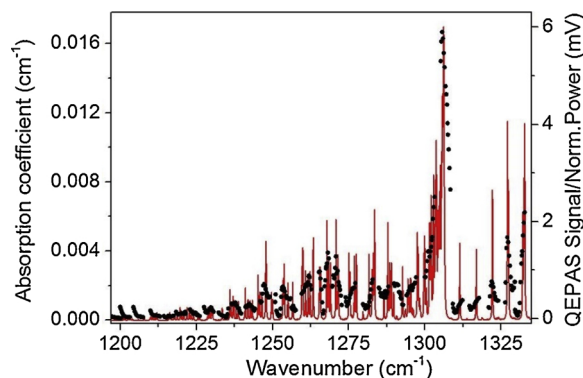

Fig. 5. Comparison between the 1000 ppm $CH_4:N_2$ TTAM QEPAS signals normalized to the optical power calibration curve (black dots, right y-axis), and the absorption spectrum simulated by using the HITRAN database (red solid lines, left y-axis).

sharp than the simulated absorption coefficient spectrum, for all the five absorption features. On the left side, the absorption features are so spectrally dense that it is hard to distinguish among them. Narrower emission linewidth (attainable with shorter laser current pulse-widths) would allow a better reconstruction of the absorption features, but the reduction of the average optical power would negatively affect the ultimate detection sensitivity of the sensor. In this mode, the spectrum acquisition time is 14 times longer, but the resolution step decreases from $4-5\,cm^{-1}$, depending on the optical frequency difference between adjacent devices, to $0.3\,cm^{-1}$, thus allowing a more accurate peaks reconstruction.

5. Methane/nitrous oxide mixtures broadband detection

The results and the sensitivities obtained so far demonstrate that the DFB-QCL array-based QEPAS sensor can be considered as a valid tool for broadband detection of one single gas species in nitrogen. A further investigation is needed to demonstrate the feasibility of broadband multi-gas detection, particularly in the case of overlapping absorption features belonging to different gas species. This is the case for nitrous oxide and methane. The absorption spectrum of N_2O has been reported in [17], where FTAM and TTAM QEPAS measurements well mimic the simulated spectrum of the P- and R-branches. These two nearly-Gaussian envelope bands overlap with uneven absorption features of CH_4 [28], within the array emission spectral range. For this experiment, three different N_2O/CH_4 mixtures in N_2 were used. A concentration of 1020 ppm of $N_2O:N_2$ in GC2 was mixed with three concentrations of $CH_4:N_2$ in GC1, containing 1900 ppm, 1000 ppm and 300 ppm of methane, in order to obtain three gas mixtures composed of a fixed concentration of 510 ppm of N_2O and a concentration of 150 ppm, 500 ppm and 950 ppm of CH_4 in N_2, respectively. Keeping the concentration of one gas species constant, it is possible to investigate how the presence of the second gas species (CH_4) can affect the overall spectrum profile.

FTAM QEPAS measurements were performed, using a lock-in phase φ fixed at 57.31°. Reference spectra measured for 510 ppm of $N_2O:N_2$, $R(\nu)_{N2O}$, and 1000 ppm of $CH_4:N_2$, $R(\nu)_{CH4}$, are shown in Fig. 6(a) and (b), respectively, while the QEPAS spectra obtained for the three different mixtures are plotted in Fig. 6(c). All spectra are normalized to the optical power calibration curve.

The presence of methane in all three mixtures clearly affects the smooth envelope of the two N_2O nearly-Gaussian absorption bands, whose QEPAS reference spectrum $R(\nu)_{N2O}$ in Fig. 6(a) is consistent with the measurements presented in [17]. By considering $R(\nu)_{CH4}$, three spectral features centered at $1266.04\,cm^{-1}$, $1306.10\,cm^{-1}$ and $1330.35\,cm^{-1}$ are clearly distinguishable. As the methane concentration increases, the presence of these bands become clearer in the mixture spectrum. In addition, in the mixture N_2O:510 ppm- CH_4:950 ppm,

a fourth spectral feature addressable to the methane contribution arises at $1251.60\,cm^{-1}$. Besides this qualitative analysis, a quantitative estimation of the amount of the two gas species in the mixture can be obtained by supposing the ith mixture spectrum, $M_i(\nu)$, as the linear combination of the two reference spectra $R_{N2O}(\nu)$ and $R_{CH4}(\nu)$. MATLAB-based software was developed to retrieve the N_2O and CH_4 concentrations in all three mixtures. The results obtained for the three gas mixtures, together with related standard errors, are summarized in Table 1.

The discrepancy between the calculated and the nominal concentration for methane decreases at higher CH_4 concentrations as well as the relative standard errors, considering its increasing contribution on the QEPAS spectrum. The discrepancy between the calculated and the nominal concentrations is below 5 % for both gases, except for methane in mixture 1, where the discrepancy is $\sim$ 6.5 %. The relative standard error of the calculated concentrations is lower than 3 % for the two gases in all the mixtures, except for the relative standard error of 6.2 % estimated for methane in mixture 1, where absorption features of methane are hardly recognizable. The obtained results prove the robustness of the QEPAS technique for a fast broadband detection of gas mixtures. However, the capability of the sensor to recognize the influence of methane absorption features on the two N_2O absorption bands is expected to improve as the acquisition spectral resolution is increased. Therefore, measurements were repeated in the TTAM configuration. The reference spectra and the three mixtures spectra are shown in Fig. 7.

The spectra in Fig. 7(c) clearly show the different contributions of the two gaseous components in the mixtures, with several methane peaks becoming visible from the N_2O P- and R-branches, even at the lowest CH_4 concentration. The N_2O and CH_4 concentrations in the three mixtures were also calculated by using the MATLAB-based software and the results are reported in Table 2.

The discrepancy between the nominal and the calculated concentration of nitrous oxide and methane is lower than 5 % for all the mixtures. Moreover, the relative standard errors of the concentrations improved of a factor ~ 2 compared to the values reported in Table 1. Compared to FTAM, TTAM measurements provide spectra with more recognizable absorption structures that can be associated to the single gas components in the mixture. Ultimately, the fitting procedure allows N_2O and CH_4 concentrations to be retrieved with a comparable level of accuracy for both acquisition modes and a higher precision is obtained in the case of operating in TTAM.

6. Conclusions

In this work we demonstrated the feasibility of broadband absorber multi-gas detection by employing a QEPAS sensor based on a DFB-QCL
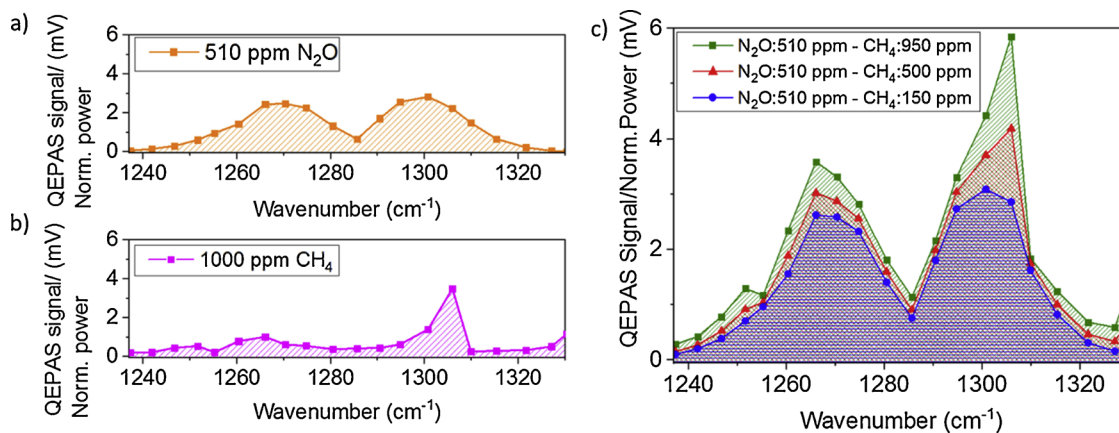

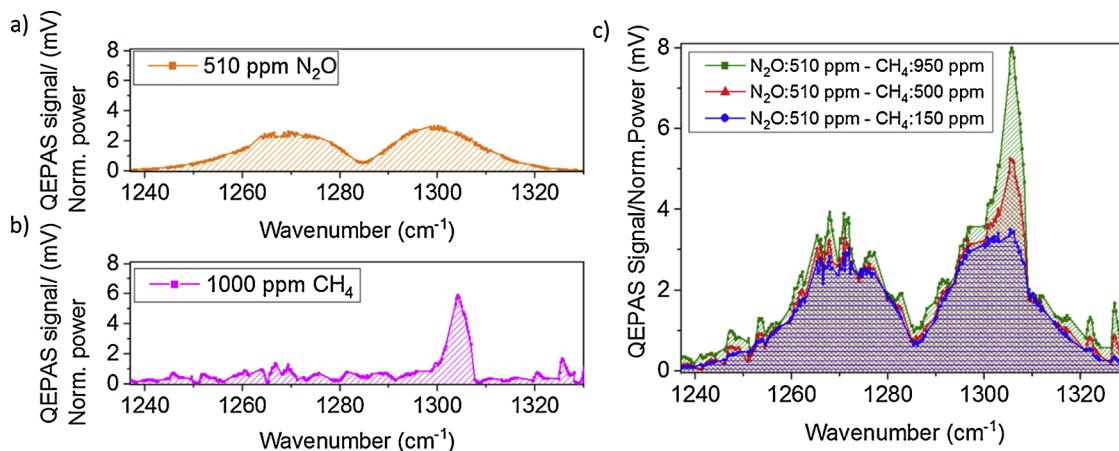**Fig. 6.** (a) 510 ppm $N_2O:N_2$ and (b) 1000 ppm $CH_4:N_2$ FTAM reference spectra; (c) FTAM QEPAS signal normalized to the optical power calibration curve for three dry mixtures containing 510 ppm of N_2O and 150 ppm of CH_4 (blue dots), 500 ppm of CH_4 (red triangles) and 950 ppm of CH_4 (green squares), respectively.

Table 1
Nominal and calculated N_2O and CH_4 concentration for the three investigated gas mixtures analyzed with FTAM QEPAS.

i	Nominal N_2O concentration (ppm)	Nominal CH_4 concentration (ppm)	Calculated N_2O concentration (ppm)	Calculated CH_4 concentration (ppm)
1	510	150	503.1 ± 3.5	159.8 ± 9.9
2	510	500	510.9 ± 4.7	504.8 ± 13.2
3	510	950	516.5 ± 6.6	947.6 ± 18.6

Fig. 7. (a) 510 ppm N_2O:N_2 and (b) 1000 ppm CH_4:N_2 TTAM QEPAS reference spectra; (c) TTAM QEPAS signal normalized to the optical power calibration curve for three dry mixtures containing 510 ppm of N_2O and 150 ppm of CH_4 (blue dots), 500 ppm of CH_4 (red triangles) and 950 ppm of CH_4 (green squares), respectively.

Table 2
Nominal and calculated N_2O and CH_4 concentration for the three investigated gas mixtures analyzed in TTAM.

i	Nominal N_2O concentration (ppm)	Nominal CH_4 concentration (ppm)	Calculated N_2O concentration (ppm)	Calculated CH_4 concentration (ppm)
1	510	150	520.9 ± 1.8	157.4 ± 4.6
2	510	500	504.6 ± 2.9	484.5 ± 7.2
3	510	950	509.8 ± 3.9	954.8 ± 9.7

array as the excitation source. The sensor architecture was determined by the spectral and beam profile characteristics of the array, leading to the choice of a 1 mm-prong spacing custom QTF as the acoustic resonator for the QEPAS sensor. The uneven methane spectrum was reconstructed within the light source emission spectral range with a spectral resolution of 0.27 cm^{-1} and 4 − 5 cm^{-1}. A methane detection sensitivity of 200 ppb was achieved with a 10 s lock-in integration time and a linear responsivity with a CH_4 concentration in the 1000 − 200 ppm range was verified. Multi-gas broadband detection was then demonstrated by analyzing three different N_2O/CH_4:N_2 mixtures in dry nitrogen within the DFB-QCL array emission spectral range. Despite the absorption spectra overlap within the whole investigated spectral range, the concentration of both gas species can be retrieved with an accuracy equal or even higher than 95 % while the precision is strongly affected by the spectral resolution of the acquisition. The two modes could be used in combination: the fast acquisition mode to determine the presence of a gas species and a slow one to retrieve its concentration with a high precision. The proof-of-concept presented in this paper represents a starting point for the development of sensors aiming at environmental monitoring of broadband greenhouse gases. In the future, investigations on the effect of relative humidity and additional interferents on the N_2O/CH_4 spectra will be performed, and multivariate analysis, like partial least squares regression, will be implemented for signal processing.

Funding

References

[1] J. Hodgkinson, R.P. Tatam, Optical gas sensing: a review, Meas. Sci. Technol. 24 (2013) 012004.

[2] P. Daukantas, Air-quality monitoring in the mid-infrared, Op. Photonics News 26 (2015) 26.

[3] M.W. Sigrist, Trace gas monitoring by laser-photoacoustic spectroscopy, Infrared Phys. Technol. 36 (1995) 415.

[4] K.C. Cossel, E.M. Waxman, I.A. Finneran, G.A. Blake, J. Ye, N.R. Newbury, Gas-phase broadband spectroscopy using active sources: progress, status, and applications, J. Opt. Soc. Am. B 34 (2017) 104.

[5] L. Xiong, W. Bai, F. Chen, X. Zhao, F. Yu, G.J. Diebold, Photoacoustic trace detection of gases at the parts-per-quadrillion level with a moving optical grating, Proc. Natl. Acad. Sci. U. S. A. 114 (2017) 7246.

[6] M. Giglio, A. Elefante, P. Patimisco, A. Sampaolo, F. Sgobba, H. Rossmadl, V. Mackowiak, H. Wu, F.K. Tittel, L. Dong, V. Spagnolo, Quartz-enhanced photoacoustic sensor for ethylene detection implementing an optimized custom tuning fork-based spectrophone, Opt. Exp. 27 (2019) 4271.

[7] A. Sampaolo, S. Csutak, P. Patimisco, M. Giglio, G. Menduni, V. Passaro, F.K. Tittel, M. Deffenbaugh, V. Spagnolo, Methane, ethane and propane detection using a compact quartz enhanced photoacoustic sensor and a single interband cascade laser, Sens. Actuator B-Chem. 282 (2019) 952.

[8] Y. Ma, Y. He, Y. Tong, X. Yu, F.K. Tittel, Ppb-level detection of ammonia based on QEPAS using a power amplified laser and a low resonance frequency quartz tuning fork, Opt. Express 25 (2017) 29356.

[9] Z. Wang, Z. Li, W. Ren, Quartz-enhanced photoacoustic detection of ethylene using a 10.5 μm quantum cascade laser, Opt. Express 24 (2016) 4143.

[10] M. Jahjah, W. Ren, P. Stefański, R. Lewicki, J. Zhang, W. Jiang, J. Tarka, F.K. Tittel, A compact QCL based methane and nitrous oxide sensor for environmental and medical applications, Analyst 139 (2014) 2065.

[11] A. Elefante, M. Giglio, A. Sampaolo, G. Menduni, P. Patimisco, V.M. Passaro, H. Wu, H. Rossmadl, V. Mackowiak, A. Cable, F.K. Tittel, Dual-gas quartz-enhanced photoacoustic sensor for simultaneous detection of methane/nitrous oxide and water

vapor, Anal. Chem. 91 (2019) 12866.

[12] G.N. Rao, A. Karpf, External cavity tunable quantum cascade lasers and their applications to trace gas monitoring, Appl. Opt. 50 (2011) A100.

[13] M.B. Pushkarsky, I.G. Dunayevskiy, M. Prasanna, A.G. Tsekoun, R. Go, C.K.N. Patel, High-sensitivity detection of TNT, Proc. Natl. Acad. Sci. U. S. A. 103 (2006) 19630.

[14] R. Lewicki, G. Wysocki, A.A. Kosterev, F.K. Tittel, QEPAS based detection of broadband absorbing molecules using a widely tunable, cw quantum cascade laser at 8.4 μm, Opt. Express 15 (2007) 7357.

[15] D. Weidmann, G. Wysocki, High-resolution broadband (& 100 cm-1) infrared heterodyne spectro-radiometry using an external cavity quantum cascade laser, Opt. Express 17 (2009) 248.

[16] B.G. Lee, M.A. Belkin, R. Audet, J. MacArthur, L. Diehl, C. Pflügl, F. Capasso, D.C. Oakley, D. Chapman, A. Napoleone, D. Bour, S. Corzine, G. Höfler, J. Faist, Widely tunable single-mode quantum cascade laser source for mid-infrared spectroscopy, Appl. Phys. Lett. 91 (2007) 231101.

[17] M. Giglio, P. Patimisco, A. Sampaolo, A. Zifarelli, R. Blanchard, C. Pfluegl, M.F. Witinski, D. Vakhshoori, F.K. Tittel, V. Spagnolo, Nitrous oxide quartz-enhanced photoacoustic detection employing a broadband distributed-feedback quantum cascade laser array, Appl. Phys. Lett. 113 (2018) 171101.

[18] https://www.epa.gov/climate-indicators/climate-change-indicators-atmospheric-concentrations-greenhouse-gases.

[19] S.L. Gerhard, D.M. Dennison, The envelopes of infrared absorption bands, Phys. Rev. 43 (1933) 197.

[20] G. Herzberg, Molecular Spectra and Molecular Structure vol. 1, Read Books Ltd., 2016.

[21] B.G. Lee, J. Kansky, A.K. Goyal, C. Pflügl, L. Diehl, M.A. Belkin, A. Sanchez, F. Capasso, Beam combining of quantum cascade laser arrays, Opt. Express 17 (2009) 16216.

[22] H. Wu, L. Dong, X. Yin, A. Sampaolo, P. Patimisco, W. Ma, L. Zhang, W. Yin, L. Xiao, V. Spagnolo, S. Jia, Atmospheric CH$_4$ measurement near a landfill using an ICL-based QEPAS sensor with VT relaxation self-calibration, Sens. Actuator B-Chem. 297 (2019) 126753.

[23] M. Giglio, P. Patimisco, A. Sampaolo, J.M. Kriesel, F.K. Tittel, V. Spagnolo, Low-loss and single-mode tapered hollow-core waveguides optically coupled with interband and quantum cascade lasers, Opt. Eng. 57 (2017) 011004.

[24] P. Patimisco, A. Sampaolo, L. Mihai, M. Giglio, J. Kriesel, D. Sporea, G. Scamarcio, F.K. Tittel, V. Spagnolo, Low-loss coupling of quantum cascade lasers into hollow-core waveguides with single-mode output in the 3.7–7.6 μm spectral range, Sensors 16 (2016) 533.

[25] P. Patimisco, A. Sampaolo, H. Zheng, L. Dong, F.K. Tittel, V. Spagnolo, Quartz enhanced photoacoustic spectrophones exploiting custom tuning forks: a review, Adv. Phys. X 2 (2016) 169.

[26] M. Giglio, P. Patimisco, A. Sampaolo, G. Scamarcio, F.K. Tittel, V. Spagnolo, Allan deviation plot as a tool for quartz-enhanced photoacoustic sensors noise analysis, IEEE Trans. Ultrason. Ferroelect. Freq. Control. 63 (2016) 555.

[27] https://www.methanelevels.org/.

[28] http://www.hitran.org/.

Marilena Giglio received the M.S. degree (cum laude) in Applied Physics in 2014, and the PhD Degree in Physics in 2018 from the University of Bari. In 2012 she's been visiting the Academic Medical Center of Amsterdam as a trainee. In 2015 she was a Research Assistant with the Department of Physics, University of Bari. She was a visiting researcher in the Laser Science Group at Rice University from 2016 to 2017. Since 2018, she is a Post-Doc Research Assistant at the Physics Department of the Technical University of Bari. Her research activity is focused on the development of gas sensors based on Quartz-Enhanced Photoacoustic Spectroscopy and on the optical coupling of hollow-core waveguides with interband- and quantum-cascade lasers.
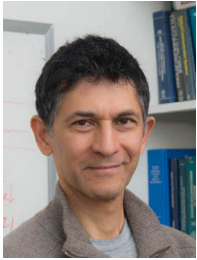
Andrea Zifarelli obtained his M.S. degree (cum laude) in Physics in 2018 from the University of Bari. From the same year, he is a PhD student at the Physics Department of the University of Bari, developing his research work at PolySense Lab, joint-research laboratory between Technical University of Bari and THORLABS GmbH. Currently, his research activities are focused on the development of gas sensors based on Quartz-Enhanced Photoacoustic Spectroscopy for detection of gas mixtures and broadband absorbers, exploiting non-conventional laser sources.

the July 2013 issue.

Angelo Sampaolo obtained his Master degree in Physics in 2013 and the PhD Degree in Physics in 2017 from University of Bari. He was a visiting researcher in the Laser Science Group at Rice University from 2014 to 2016. Since May 2017, he is a Post-Doctoral Research associate at University of Bari. His research activity has included the study of the thermal properties of heterostructured devices via Raman spectroscopy. Most recently, his research interest has focused on the development of innovative techniques in trace gas sensing, based on Quartz-Enhanced Photoacoustic Spectroscopy and covering the full spectral range from near-IR to THz. His achieved results have been acknowledged by a cover paper in Applied Physics Letter of

Giansergio Menduni received the M.S. degree (cum laude) in Electronic Engineering in 2017 from the Technical University of Bari. Since 2018, he is a PhD student at the Electric and Information Engineering Department of the Technical University of Bari. His research activity is focused on the development of gas sensors based on Quartz-Enhanced Photoacoustic Spectroscopy.

Arianna Elefante received her M.S. degree (cum laude) in Physics in 2016 from the University of Bari. Since 2017, she is a PhD student at the Physics Department of the University of Bari. Her research activity is conducted in collaboration with THORLABS GmbH and is focused on the development of gas sensors based on Quartz-Enhanced Photoacoustic Spectroscopy for the simultaneous detection of two gas species.

Dr. Romain Blanchard received his PhD in Applied Physics in the group of Federico Capasso at Harvard University and his MS from Ecole Polytechnique in Paris, France. His doctoral studies focused on wavelength control and beam engineering of quantum cascade lasers, as well as novel nano-optics technologies. Dr. Blanchard joined Eos Photonics in 2013 as a Senior Scientist and at Pendar Technologies he leads the design of new products and solutions and oversees internal R&D efforts and government programs.

Dr. Christian Pfluegl received his PhD in Electrical Engineering in 2005 from the Vienna University of Technology, Austria and his MS in Applied Physics from the University of Regensburg, Germany in 2002. From 2006 to 2010, he worked as a Research Associate at Harvard University in the group of Prof. Federico Capasso. His PhD and postdoctoral work focused on the development of Quantum Cascade Laser (QCL) technology and QCL-based instruments. In 2010, he co-founded Eos Photonics, where he served as VP of R&D and later as COO. At Pendar Technologies, he oversees the development and commercialization of QCL array technology.

Dr. Mark F. Witinski completed his doctorate in Chemical Physics at Cornell University in 2006, where his work centered on using molecular beams and laser spectroscopy to examine the dynamics of molecular collisions. He then spent over five years as a Research Associate in the laboratory of Prof. Jim Anderson at Harvard University. There, he was focused on innovative approaches to Mid-IR spectroscopy using Quantum Cascade Lasers. He is a Fulbright Scholar. Dr. Witinski served as co-founder and President of Eos Photonics. At Pendar Technologies, he focuses primarily on applications development, business-to-business strategic partnerships, and government sales.

Dr. Daryoosh Vakhshoori is the founder, CEO and President of Pendar Technologies. He received his BS from the University of California at Irvine and holds a PhD in Quantum Electronics from the University of California at Berkeley. He was a research scientist at AT&T Bell Laboratories, later Lucent Technologies. Dr. Vakhshoori was a co-founder of CoreTek, Inc. (1996–2002), a high-tech company that developed novel tunable laser and optical filters for the telecommunication market based on micro-electromechanical technology. He founded Ahura Scientific (2002–2010), with the aim of moving advanced spectroscopic techniques out of scientific laboratories into the hands of non-specialist field operators. In 2010, Thermo Fisher Scientific acquired the company. Dr. Vakhshoori founded Pendar in 2011 to create intelligent chemistry systems.

Hongpeng Wu received his Ph.D. degree in atomic and molecular physics from Shanxi University, China, in 2017. From September, 2015 to October, 2016, he worked as a joint PhD. student in the Electrical and Computer Engineering Department and Rice Quantum Institute, Rice University, Houston, USA. Currently he is an associate professor in the Institute of Laser Spectroscopy of Shanxi University. His research interests include optical sensors, trace gas detection, and laser spectroscopy.

Vittorio M. N. Passaro received the Laurea degree (cum laude) in electronic engineering from the University of Bari, Bari, Italy, in 1988, and the Ph.D. degree in electronic engineering from the Politecnico di Bari, Bari, Italy, in 1992. Since October 2000, he joined the Politecnico di Bari as an Associate Professor of electronics. Since 2004, he has been the founder and the leader of the Photonics Research Group, Politecnico di Bari. He is an author or coauthor of more than 370 papers in optoelectronics and photonics topics, published in international journals (one by Nature Photonics) and conference proceedings. He holds two international patents and is the editor of five scientific books (one by Springer).

Pietro Patimisco obtained the Master degree in Physics (cum laude) in 2009 and the PhD Degree in Physics in 2013 from the University of Bari. Since 2018, he is Assistant professor at the Technical University of Bari. He was a visiting scientist in the Laser Science Group at Rice University in 2013 and 2014. Dr. Patimisco's scientific activity addressed both micro-probe optical characterization of semiconductor optoelectronic devices and optoacoustic gas sensors. Recently, his research activities included the study and applications of trace-gas sensors, such as quartz-enhanced photoacoustic spectroscopy and cavity enhanced absorption spectroscopy in the mid infrared and terahertz spectral region, leading to several publications, including a cover paper in Applied Physics Letter of the July 2013 issue.

Frank K Tittel obtained his bachelor, master, and doctorate degrees in physics from the University of Oxford in 1955 and 1959, respectively. From 1959 to 1967, he was a Research Physicist with General Electric Research and Development Center, Schenectady, New York. Since 1967 he has been on the faculty of the Department of Electrical and Computer Engineering and Biomedical Engineering at Rice University in Houston, TX, where he currently an Endowed Chaired Professor. Current research interests include various aspects of quantum electronics, in particular laser spectroscopy and laser applications in environmental monitoring, atmospheric chemistry, industrial process control, and medical diagnostics. Dr. Tittel is a Fellow of the IEEE, Optical Society of America, the American Physical Society and SPIE.

Lei Dong received his Ph.D. degree in optics from Shanxi University, China in 2007. From June, 2008 to December, 2011, he worked as a post-doctoral fellow in the Electrical and Computer Engineering Department and Rice Quantum Institute, Rice University, Houston, USA. Currently he is a professor in the Institute of Laser Spectroscopy of Shanxi University. His research interests include optical sensors, trace gas detection, and laser spectroscopy.

Vincenzo Spagnolo obtained the PhD in physics in 1994 from University of Bari. From 1997 to 1999, he was researcher of the National Institute of the Physics of Matter. Since 2004, he works at the Technical University of Bari, formerly as assistant and associate professor and, starting from 2018, as full Professor of Physics. He is the director of the joint-research lab PolySense between Technical University of Bari and THORLABS GmbH, fellow member of SPIE and senior member of OSA. His research interests include optoacoustic gas sensing and spectroscopic techniques for real-time monitoring. His research activity is documented by more than 190 publications and two filed patents. He has given more than 50 invited presentations at international conferences and workshops.